High-resolution Multiband Passive Polarimetric Observations of the Ocean Surface

Jeffrey R. Piepmeier and Albin J. Gasiewski
School of Electrical and Computer Engineering
Georgia Institute of Technology, Atlanta, GA 30332-0250
(404) 894-2984; (404) 894-2934; FAX (404) 894-4641
gt2930b@prism.gatech.edu; ag14@prism.gatech.edu

Abstract - A multiband microwave polarimetric scanning radiometer (PSR) was operating during January-March, 1997 over the Labrador Sea and the Atlantic Ocean aboard the NASA/WFF P-3B aircraft. Conically-scanned brightness temperatures were observed over open ocean for a variety of wind speeds and cloud conditions. Presented here are several illustrations and applications of data obtained during the Labrador Sea experiment.

INTRODUCTION

A versatile new airborne microwave imaging radiometer, the Polarimetric Scanning Radiometer (PSR), has been developed for the purpose of obtaining polarimetric microwave emission imagery of the Earth's oceans, land, ice, and clouds and precipitation [1]. In early 1997, the PSR was integrated onto the NASA Wallops Flight Facility P-3B Orion (N426NA) in conjunction with the Ocean Winds Imaging (OWI) Labrador Sea experiment. During the Labrador Sea deployment, conical, cross-track, and fixed-angle stare scanning modes where used to obtain calibrated brightness temperature data over a wind-driven ocean. Here, data from the experiment is used to illustrate the various scan modes available using the PSR.

INSTRUMENT DESCRIPTION

The PSR consists of a set of four tri-polarimetric ($T_v \sim \langle|E_v^2|\rangle$, $T_h \sim \langle|E_h^2|\rangle$, $T_U \sim 2\Re\langle E_v E_h^*\rangle$) radiometers housed within a cylindrically shaped gimbal-mounted scanhead. The scanhead contains an 80486 PC, an eight-channel digital correlator bank, and four total-power tri-polarimetric radiometers. The radiometric bands measured are X (10.6-10.8 GHz), K (18.5-18.9 GHz), Ka (36-38 GHz), and W (86-92 GHz). These bands are selected to provide sensitivity to clouds, precipitation, and surface features over almost one decade of microwave spectrum at octave intervals. The radiometer antennas are orthogonal linearly-polarized corrugated feedhorns with grooved rexolite lenses. A single dual-band antenna is used for the X- and Ka-band channels. Antenna diameters are chosen to provide beamwidths of 8^o (for both X- and K-bands) and 2.3^o (for both Ka- and W-bands.) Main beam efficiencies are greater than 0.95 and on-axis cross-polarization discrimination exceeds 27 dB. Fig. 1 is a video image showing the PSR in the P3 bomb-bay – the antenna lenses are clearly visible. The scanhead is rotatable by the positioner so that the radiometers can view any angle within 70^o elevation of nadir and any azimuth angle (a total of 1.32π sr solid angle), as well as external hot and ambient calibration targets. This configuration supports conical, cross-track, along-track, fixed-angle stare, and spotlight scan modes.

LABRADOR SEA EXPERIMENT

During the Labrador Sea experiment, the PSR was operated in three scan modes (conical, cross-track, and fixed angle stare) over ocean, land, and sea ice. The conical scan mode was used over ocean to obtain azimuthal scans of the wind-driven surface. The cross-track mode was used to estimate elevational brightness temperature profiles, and the fixed angle stare mode was used to obtain views of the cold sky for an extra calibration point.

Conical scanning

Azimuthal variations of the wind-driven ocean surface were observed using the conical scan mode. For a single straight and level flight track on March 4, 1997, nineteen azimuthal scans were averaged to arrive at a mean azimuthal signature for vertical and horizontal polarizations at X- and K-bands. The surface conditions according to the *R.V. Knorr* were winds from 270^o at 15 m/s gusting to 17 m/s with a 5-meter swell from 275^o. Fig.s 2-5 show the brightness temperature variations for the four channels. The signatures display the expected $sin(\phi)$ and $sin(2\phi)$ variations as observed in both SSM/I data [2] and in simulations using an asymmetric wave geometric optics model [3]. Furthermore, the variations exhibit the expected phase associated with an upwind brightening in T_v and a null in T_h.

Cross-track scanning

A useful function for computing pitch and roll corrections to brightness temperatures is the derivative of brightness temperature with respect to elevation angle. Although $dT_B/d\theta$ can be computed using radiative trans-

Band	Polarization	$dT_B/d\theta$ (K/^{o})
X	V	1.83
X	H	-1.02
K	V	2.36
K	H	-0.87
Ka	V	2.25
Ka	H	-0.71
W	V	-0.58
W	H	1.06

Table 1: Elevation brightness correction coefficients (winds at 15 m/s, cloud ceiling at 2km.)

fer theory, an in-situ measurement is invaluable due to specific surface conditions and cloud layers that are not easily characterized for inclusion in a radiative transfer model. Performing cross-track scans coupled with an aircraft spiral maneuver allows the entire hemisphere of surface incident angles to be sampled. From this data set an azimuthally averaged brightness temperature elevation profile is easily produced. Having executed this a number of times during the deployment, an example from March 4, 1997 is reported here. Sea surface conditions are identical to those reported in the previous section. Additionally, upon aircraft descent, the cloud tops are observed at two km altitude. A plot for T_v at Ka-band is given in Fig. 6. This curve is calculated by averaging ten cross-track scans as the aircraft executed a partial circle banked at 20^o. The slope of this curve at 53.1 degrees from nadir yields the desired $dT_B/d\theta$ for aircraft attitude correction of conically scanned brightness temperature data taken at the standard SSM/I incident angle. The values of these correction coefficients are shown for all PSR bands at vertical and horizontal polarizations in Table 1.

Fixed-angle stare

Physical temperature gradients and the off normal incidence view angle of the hot and cold calibration targets cause the emission temperatures of the loads to be slightly lower than the measured physical temperatures. This causes an additional unknown, an effective emissivity of the targets, in the calibration relationship. The emission temperature of a calibration load in thermal equilibrium is

$$T_{emiss} = T_{amb} + \epsilon_{eff}(T_{load} - T_{amb}),$$

where T_{emiss}, T_{amb}, and T_{load} are the emission temperature, ambient temperature, and load's heatsink temperature, respectively. With a third calibration data point, the additional parameter may be determined. This third point must be taken in-situ when the aircraft is at normal operational altitude and the microwave absorbing material is in thermal equilibrium. Above the clouds, the view of a cold sky presents itself as an excellent third calibration point. With the antennas pointed to 60^o above aircraft nadir, the aircraft rolls an additional 60^o, resulting in a look at the cold sky 30^o above the horizon (or 120^o from nadir.) The cold sky look coupled with hot and cold calibration load looks forms a three point data set. The optimal value of ϵ_{eff} is found by varying this parameter to affect a minimum sum of squared-errors for a best-fit line through the three calibration points. For the flight on March 7, 1997, the effective emissivity is estimated to be approximately 0.7 for all channels. This is reasonable considering the strong temperature gradients expected within the microwave absorber which comprises the calibration targets.

CONCLUSION

In conclusion, these data excerpts from the Labrador Sea deployment demonstrate the usefulness of a scanning polarimetric radiometer for ocean wind studies. Further work remains in data processing, particulary the calibration and processing of the correlation channel for determination of T_U, for further understanding of passive high wind-speed signatures. Future deployments of the PSR are planned to provide an expanded data base with which to study ocean and atmospheric thermal emission.

ACKNOWLEDGMENTS

The authors wish to thank C. Campbell, E. Thayer, R.C. Lum, M. Klein, and D. DeBoer for their assistance in the PSR integration and operation phases; and are grateful for support from the following organizations: U.S. Office of Naval Research (grants N00014-95-1-0426 and N00014-95-1-1007), NASA Headquarters (grant NAGW-4191), and the NPOESS Integrated Program Office (contract SMC 185-96-N0109).

REFERENCES

[1] J. R. Piepmeier and A. J. Gasiewski, "Polarimetric scanning radiometer for airborne microwave imaging studies", in *Proc. 1996 Int. Geosci. and Remote Sens. Symp. (IGARSS)*, University of Nebraska, Lincoln, NE, 1996, pp. 1688–1691.

[2] F. J. Wentz, "Measurement of oceanic wind vector using satellite microwave radiometers", *IEEE Trans. Geosci. Remote Sens.*, vol. 30, no. 5, pp. 960–972, September 1992.

[3] D. B. Kunkee and A. J. Gasiewski, "Simulation of passive microwave wind direction signatures over the ocean using an asymmetric-wave geometrical optics model", *Radio Science*, vol. 32, no. 1, pp. 59–77, 1997.

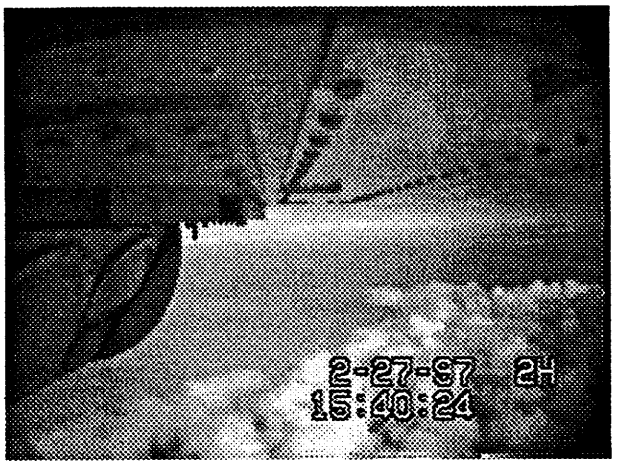

Figure 1: PSR on NASA WFF P3-B, aft view.

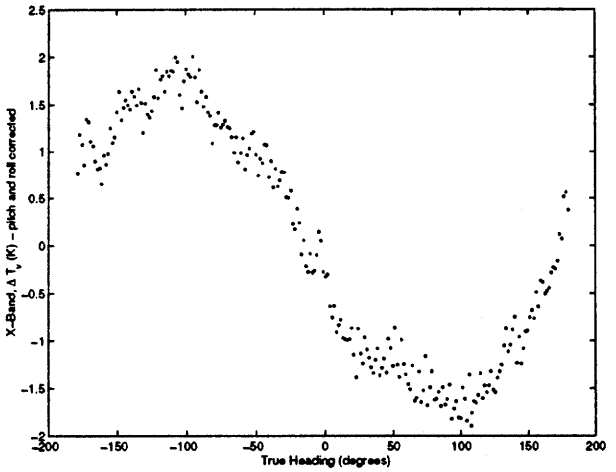

Figure 2: X-band ΔT_v averaged over 19 azimuthal scans. The wind direction is reported to be from -90° .

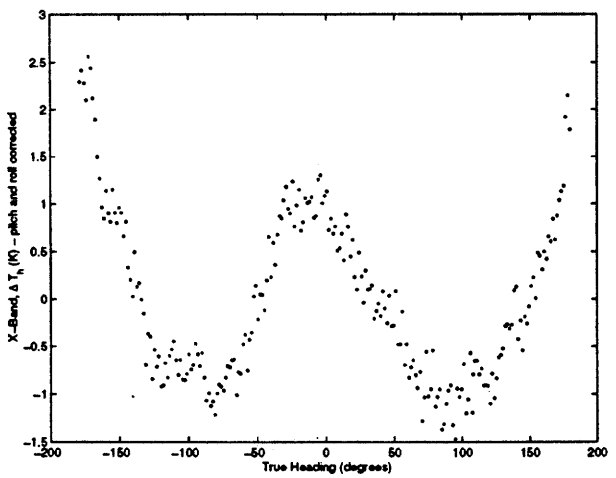

Figure 3: X-band ΔT_h averaged over 19 azimuthal scans.

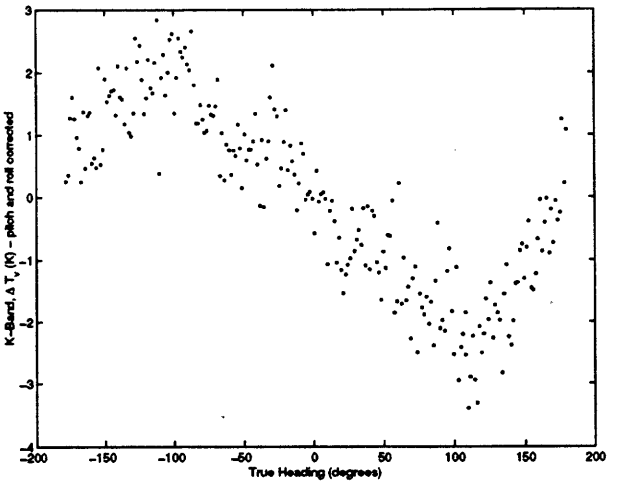

Figure 4: K-band ΔT_v averaged over 19 azimuthal scans.

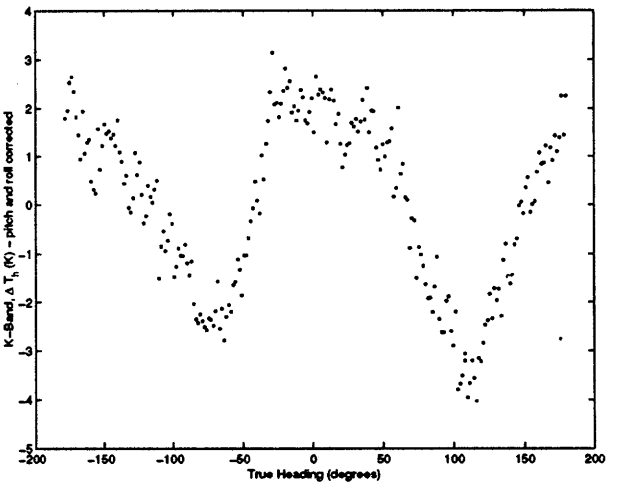

Figure 5: K-band ΔT_h averaged over 19 azimuthal scans.

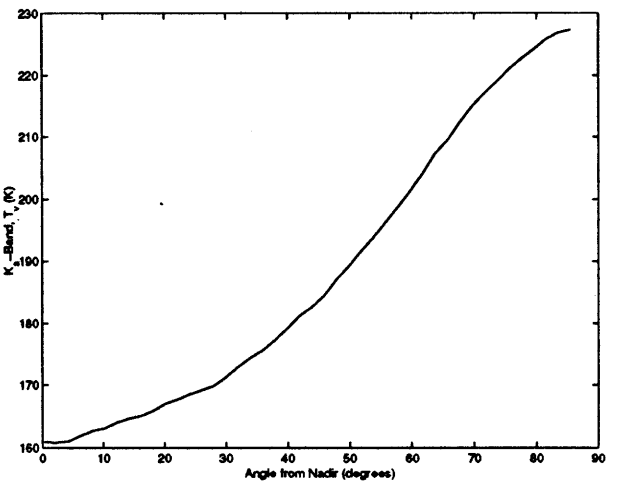

Figure 6: Ka-band T_v elevational profile.